Behavioral/Cognitive

Common and Unique Neurophysiological Processes That Support the Stopping and Revising of Actions

Mario Hervault[1,2,3] **and Jan R. Wessel**[1,2,3]

[1]Department of Psychological and Brain Sciences, University of Iowa, Iowa City, Iowa 52242, [2]Department of Neurology, University of Iowa Hospitals and Clinics, Iowa City, Iowa 52242, and [3]Cognitive Control Collaborative, University of Iowa, Iowa City, Iowa 52242

Inhibitory control is a crucial cognitive-control ability for behavioral flexibility, which has been extensively investigated through action-stopping tasks. Multiple neurophysiological features have been proposed as "signatures" of inhibitory control during action-stopping, though the processes indexed by these signatures are still controversially discussed. The present study aimed to disentangle these processes by comparing simple stopping situations with those in which additional action revisions were needed. Three experiments in female and male humans were performed to characterize the neurophysiological dynamics involved in action-stopping and action-changing, with hypotheses derived from recently developed two-stage "pause-then-cancel" models of inhibitory control. Both stopping and revising an action triggered an early, broad "pause"-process, marked by frontal EEG β-frequency bursting and nonselective suppression of corticospinal excitability. However, EMG showed that motor activity was only partially inhibited by this "pause" and that this activity could be modulated during action revision. In line with two-stage models of inhibitory control, subsequent frontocentral EEG activity after this initial "pause" selectively scaled depending on the required action revisions, with more activity observed for more complex revisions. This demonstrates the presence of a selective, effector-specific "retune" phase as the second process involved in action-stopping and action revision. Together, these findings show that inhibitory control is implemented over an extended period of time and in at least two phases. We are further able to align the most commonly proposed neurophysiological signatures to these phases and show that they are differentially modulated by the complexity of action revision.

Key words: **cognitive control; corticospinal excitability; EEG; EMG; inhibitory control; stop-signal task**

Significance Statement

Inhibitory control is one of the most important control processes by which humans can regulate their behavior. Multiple neurophysiological signatures have been proposed to index inhibitory control. However, these play out on different time scales and appear to reflect different aspects of cognitive control, which are controversially debated. Recent two-stage models of inhibitory control have proposed that two phases implement the revisions of actions: "pause" and "retune." Here, we provide the first empirical evidence for this proposition: action revisions engendered a common, low-latency "pause" process, during which motor activity is broadly suppressed. Later activity, however, distinguishes between simple stopping of actions and more complex action revisions. These findings provide novel insights into the sequential dynamics of human action control.

Introduction

Inhibitory control is a core cognitive control ability that permits the revision of an already-initiated action, for example, during rapid environmental changes. Over the past decades, its neural basis and clinical relevance have been extensively investigated based on action-stopping tasks (Logan and Cowan, 1984; Verbruggen et al., 2019). Multiple neurophysiological signatures of inhibitory control during action-stopping have been proposed (Huster et al., 2013; Wessel and Aron, 2017; Jana et al., 2020). They include the reduction of residual EMG activity on successfully stopped actions (partial-response EMG; prEMG; Raud et al., 2022), corticospinal excitability (CSE) suppression (Duque et al., 2017), frontocentral β-bursts (Wessel, 2020), the P3 ERP (Wessel and Aron, 2015), and frontocentral θ power (Messel et al., 2021). It has been a major challenge to reconcile these signatures under a common theoretical framework, especially since they occur at

Received May 29, 2024; revised Jan. 8, 2025; accepted Jan. 24, 2025.

Author contributions: M.H. and J.R.W. designed research; M.H. performed research; M.H. analyzed data; M.H. and J.R.W. wrote the paper.

This work was supported by National Science Foundation Career Grant 1752355 to J.R.W. and National Institutes of Health Grant R01 NS117753 to J.R.W. We thank all the volunteers for their participation and Nathan Chalkley, Nathan Chen, and Saara Engineer for their help in data acquisition.

The authors declare no competing financial interests.

Correspondence should be addressed to Mario Hervault at mario.hervault@univ-grenoble-alpes.fr.

https://doi.org/10.1523/JNEUROSCI.1537-24.2025

Copyright © 2025 the authors

different times after the signal to stop. Moreover, several signatures have been challenged with regard to their relationship to inhibitory control altogether (see Huster et al., 2020; Skippen et al., 2020; Hervault et al., 2025 for review).

To account for this inconsistency, recently proposed "pause-then-cancel" (PTC) models (Schmidt and Berke, 2017; Diesburg and Wessel, 2021) have conceptualized inhibitory control as a two-stage dynamic. An early "pause" process is triggered by any unexpected signal to implement quick (~150 ms) and broad inhibition of the motor system. This process has been proposed to be reflected in nonselective CSE suppression and the early suppression of prEMG (Tatz et al., 2021; Wessel et al., 2022). Additionally, β-bursts dynamics have been proposed to reflect subcortical–cortical communication (Diesburg et al., 2021) in a time frame corresponding to the "pause" stage (Hannah et al., 2020; Tatz et al., 2023; Wadsley et al., 2023a). This "pause" ostensibly buys time for a second process ("cancel") to stop the action in a selective fashion that depends on the task requirement (Tatz et al., 2021; Waller et al., 2021). Frontocentral P3 ERP and θ power increase have been proposed to index this process (Diesburg and Wessel, 2021). In addition, it has been proposed that the "cancel" stage reflects a stop-specific instantiation of a more general "retuning" process. In other words, "cancel" only means "cancel" if the task requires a complete cessation of all responding. If more complex adjustments are necessary, these "cancel"-process signatures should parametrically scale with the complexity of the response revision and should reflect a "retuning" of the response rather than its cancellation (Diesburg and Wessel, 2021).

The current study aimed to comprehensively investigate these predictions regarding the purported neurophysiological signatures of inhibitory control under the human PTC model. We designed a series of tasks in which actions had to be revised with different degrees of complexity. Based on the PTC model, we predicted that markers of the "pause" stage (CSE suppression, prEMG, and frontal β-bursts) would be shared between all action-stopping and action-changing requirements. Crucially, however, we predicted that purported markers of the "cancel" stage (frontocentral P3 and θ power) would scale with the required response revision (stopping, changing one response dimension, changing two response dimensions). This would confirm a key theoretical proposal of a more generic "pause-then-retune" dynamic for action revision (Diesburg and Wessel, 2021).

Alternatives to these hypotheses are at least twofold. First, action-changing might engage inhibitory processing more selectively than action-stopping (De Jong et al., 1995; Antons et al., 2019). If so, "pause"-stage signatures should not be observed (or be reduced) during action-changing. Second, previous fMRI studies (Kenner et al., 2010; Boecker et al., 2011) have identified that cortical blood oxygenation level-dependent (BOLD) responses in action-changing were similar to the sum of the BOLD responses in action-stopping and action-initiation. This suggested that action-changing was performed by the sum of a generic stopping process plus a new response triggering (Boecker et al., 2013). If so, the "cancel" stage purported signatures should index a similar inhibition dynamic across stopping and changing.

Together, this comprehensive investigation aims to test the validity of the recent neurocognitive models of inhibitory control, address contradictory unitary/dissociated views of stopping and changing processing (Krämer et al., 2011; Boecker et al., 2013; Rangel-Gomez et al., 2015; Elchlepp and Verbruggen, 2017), and understand specific clinical impairments in action-changing (McClure et al., 2005; Roberts and Husain, 2015; van den Wildenberg et al., 2017).

Experiment 1

Materials and Methods

Hypothesis. Our main hypothesis for Experiment 1 was that both action-stopping and action-changing would induce short-latency CSE suppression, suggesting that a nonselective "pause" inhibition dynamic is engaged in both situations. Stopping and changing have been investigated in mixed task blocks (Boecker et al., 2007, 2011; Drueke et al., 2010; Rangel-Gomez et al., 2015). However, by intermixing STOP and STOP-CHANGE trials, one could bias the STOP-CHANGE condition toward exhibiting the same nonselective inhibition found during stopping, as participants may stop all responses first while they discern between stop and change signals (Bissett and Logan, 2014; Giarrocco et al., 2021). To allow a stronger test of the hypothesis that action-stopping and action-changing would share this initial nonselective inhibitory phase, we hence tested them in separate blocks, allowing participants to use their preferred strategy for either behavior.

Participants. Twenty-four healthy individuals (15 females; mean age 19 years; SD = 1.6) participated in the experiment in exchange for course credit or an hourly payment of $15. They completed transcranial magnetic stimulation (TMS) screening questions (Rossi et al., 2011) and provided written informed consent. Procedures were approved by the local Institutional Review Board (IRB number 201612707) and conducted in accordance with the Declaration of Helsinki.

Boecker et al. reviewed 10 experiments comparing STOP signal versus STOP-CHANGE signal reaction times ($SSRT_{STOP}$, $SSRT_{STOP\text{-}CHANGE}$) in groups of healthy participants ranging from 8 to 24 individuals (Boecker et al., 2013). We thus targeted 24 participants as the upper range of the previously reported experiments.

Experimental task. The task design followed recent guidelines for stopping tasks procedures (Verbruggen et al., 2019). The participants performed a randomized sequence of STOP-task blocks and STOP-CHANGE–task blocks involving foot responses within a single session. The behavioral task was presented on a Linux desktop computer based on Matlab 2017a (The MathWorks) custom scripts, including Psychophysics Toolbox functions (Brainard, 1997). The task design is depicted in Figure 1. The stimuli were displayed centrally on a black background screen. The main GO task was a two-choice reaction–time task. In each trial, after a fixation cross was displayed for a random duration ranging from 400 to 700 ms, a white arrow pointing to the left or the right direction was displayed as the GO stimulus. Participants were instructed to respond quickly and accurately to the GO stimulus by pushing the corresponding left or right foot pedal on a Kinesis Savant Elite 2 response device. In a pseudorandomly chosen 1/3 of the trials, the white arrow (GO) turned into a STOP or STOP-CHANGE signal after a variable delay (see below). The STOP signal was a blue rectangle instructing participants to try to stop the initial GO response. The STOP-CHANGE signal was a blue arrow pointing in the opposite direction instructing participants to try to stop the initial GO response and, instead, push the opposite foot pedal. Therefore, the STOP-CHANGE instruction included both the requirement to stop the initial response and an additional demand to replace it with another response. The STOP/STOP-CHANGE signal delay (SSD) between the onset of the GO stimulus and the STOP/STOP-CHANGE signal display, initially set to 200 ms, was dynamically adjusted in 50 ms increments to achieve a probability of responding to the initial GO stimulus p(resp|signal) of ~0.50 in signal trials. If the participant completed the initial GO response after a STOP/

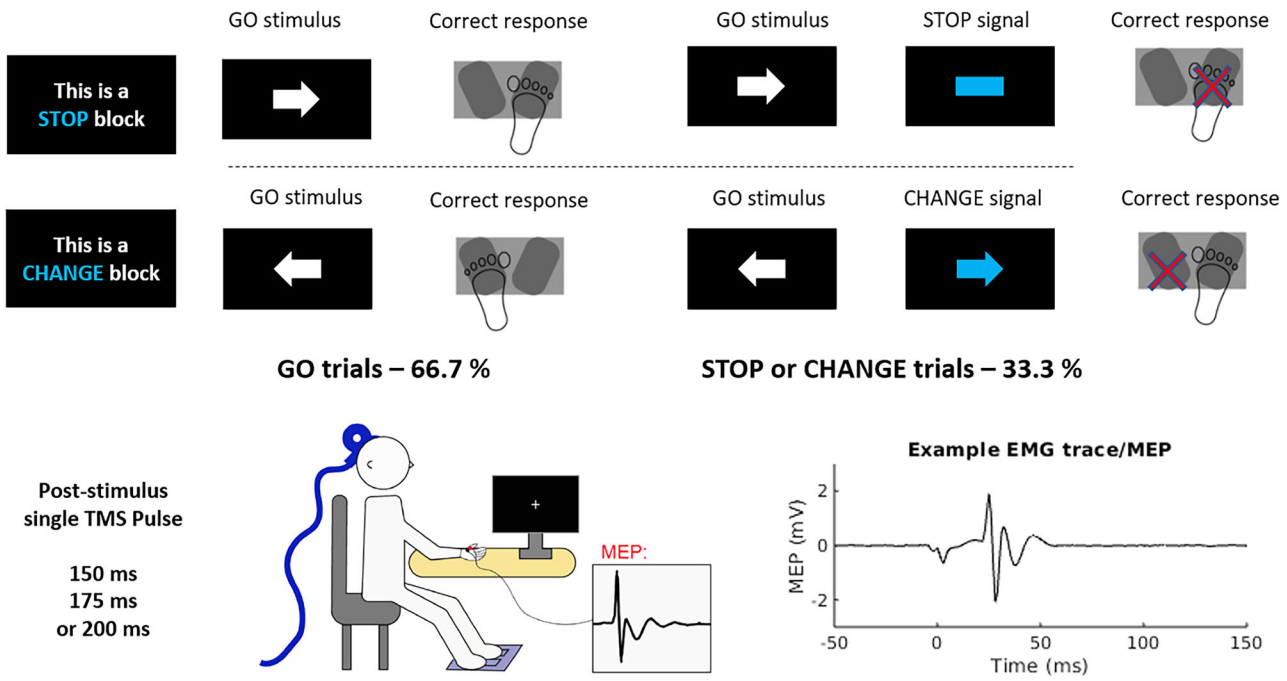

Figure 1. Task diagram of Experiment 1. Top, Time course of the behavioral task. Following the presentation of the GO stimulus, the arrow changed to blue in a minority of trials (33.3%). These signaled to the participant to try to stop their initial response (STOP signal) or to stop the initial response by changing it with the newly instructed response (STOP-CHANGE signal). Bottom, The setup involved recording MEP from the right hand, while the feet were used to respond (see main text for details of the EMG montage). Example of MEP trace from one participant to Experiment 1 (Subject 10, STOP block, GO trial, TMS pulse 150 ms). MEP trace is locked to the TMS stimulation (time, 0 ms).

STOP-CHANGE signal presentation, the trial was considered unsuccessful, and the SSD was shortened in the next signal trial (US, unsuccessful STOP; UC, unsuccessful STOP-CHANGE). Otherwise, if the initial GO response was canceled, the trial was considered successful, and the SSD was lengthened in the next signal trial (SS, successful STOP; SC, successful STOP-CHANGE). The incremental SSD adjustment was specific to the block type (stopping or changing) and to the responding foot (left or right). If the RT to the GO stimulus or STOP-CHANGE signal was above 1,000 ms, the feedback "Too slow!" was displayed on the screen for a 1,300 ms duration. Overall, the duration between two subsequent GO stimuli was 3,600 ms.

Participants performed 12 blocks of 90 trials (60 GO trials + 30 STOP/STOP-CHANGE signal trials). Instructions for the upcoming block (either STOP-task or STOP-CHANGE-task block) were displayed before each block initiation. Blocks started with a sequence of three consecutive GO trials and were concluded by written and verbal feedback including the block average GO trial RT (GO-RT) and p(resp|signal). To maintain a p(resp|signal) close to 0.50 and between 0.40 and 0.60, the participants were encouraged either to speed up their GO-RT or to increase their successful stopping/changing rate. A minimum of two practice blocks (stopping and changing), 30 trials each (10 signal trials), were performed before the actual experiment. This practice was repeated if the p(resp|signal) was outside the 0.40–0.60 range. White and blue color correspondence to GO stimuli and STOP/STOP-CHANGE signals was randomized across participants.

TMS/MEP procedures. CSE was assessed based on an EMG measure of the motor-evoked potential (MEP) induced by a single TMS pulse. As we use the MEP to investigate a nonselective inhibition process, it was quantified from the right index finger as a task-irrelevant effector (Badry et al., 2009; Majid et al., 2012; Wessel et al., 2013).

EMG was measured using a bipolar belly–tendon montage from the right first-dorsal interosseous muscle using adhesive electrodes (H124SG, Covidien) and a ground electrode placed over the distal end of the ulna bone. EMG electrodes were passed through a Grass P511 amplifier (Grass Products) and sampled using a CED Micro 1401-3 sampler (Cambridge Electronic Design) and CED Signal software. EMG was sampled at a rate of 1,000 Hz with online 30 Hz high-pass, 1,000 Hz low-pass, and 60 Hz notch filters—note that while much past work from us and others used notch filtering for the purposes of MEP research (Claffey et al., 2010; Majid et al., 2012; Tatz et al., 2021) and while notch filtering increases the SNR of the MEP (Nikolov et al., 2021), others have not used notch filtering during the recording (Wadsley et al., 2023b). EMG sweeps were triggered 90 ms before each TMS pulse, and EMG was recorded for 1,000 ms. TMS was delivered via a MagStim 200-2 system (MagStim) with a 70 mm figure-of-eight coil. Before the experimental task, hotspotting was used to identify the correct location and intensity for each participant. The coil was initially located 5 cm left of and 2 cm anterior to the vertex. Location and stimulation intensity were incrementally adjusted to identify the participant's resting motor threshold. Resting motor threshold was the minimum intensity needed to produce MEPs >0.1 mV in 5 of 10 consecutive probes (Rossini et al., 1994). For the main experiment, the stimulus intensity was increased to 115% of resting motor threshold. The mean experimental intensity was 62% (SD = 7.6%) of maximum stimulator output.

Participants completed 1,080 trials. In 1/3 of GO trials ($n = 240$), as well as every STOP ($n = 180$) and STOP-CHANGE trial ($n = 180$), a TMS pulse was delivered randomly at one of the three following latencies: 150 ms, 175 ms, and 200 ms (resulting in $n = 60$ trials per signal type for a given latency). The TMS pulse latencies were chosen based on previous work establishing MEP suppression as a marker of nonselective

inhibition through the corticosubcortical hyperdirect pathway (Tatz et al., 2021; Wessel et al., 2022). The MEPs from these TMS pulses of interest were normalized based on another set of GO trials (1/3 of the GO trials, $n = 240$) on which the TMS pulse was delivered 50 ms prior to the GO stimulus display to reflect an "active baseline MEP" (i.e., reflecting CSE during intertrial interval). The last 1/3 of the GO trials were TMS pulse-free ($n = 240$).

Data analyses. GO_{STOP}-RT and GO_{CHANGE}-RT were computed as the mean GO-RT from STOP and STOP-CHANGE blocks, respectively. US-RT and UC-RT were computed as the mean RT of unsuccessful STOP trials and unsuccessful STOP-CHANGE trials (STOP-CHANGE trials in which the original response was executed), respectively. GO2-RT was also computed as the mean RT to the STOP-CHANGE signal when changing was successful. Participants' behavioral inhibition latencies (STOP/STOP-CHANGE signal RT), $SSRT_{STOP}$ and $SSRT_{CHANGE}$, were estimated using the integration method with replacement of GO omissions (Verbruggen and Logan, 2009; Verbruggen et al., 2019). This consisted of subtracting the mean SSD from the nth RT, where n equals the number of GO-RTs multiplied by the overall p(resp|signal). Blocks with a p(resp|signal) outside the 0.30–0.70 range were excluded. Overall, this was the case for three STOP blocks (across three participants) and three STOP-CHANGE blocks (across two participants). Trials with a GO-RT or GO2-RT shorter than 150 ms or longer than 1,000 ms were also removed. The average number of removed trials per participant was 2.3 (SD = 6.3) for stopping and 2.9 (SD = 6.8) for changing.

The MEP amplitude was extracted semiautomatically from the EMG trace using ezTMS, a freely available TMS preprocessing tool developed for use in MATLAB (Hynd et al., 2021; Tatz et al., 2021). The MEP amplitude was defined as the difference between the maximum and minimum amplitude 10–50 ms after the TMS pulse. In addition to automatically determining the MEP amplitude, each trial was visually inspected for accuracy without knowledge of the specific trial type. Trials in which the MEP amplitude was <0.01 mV or the root mean square (RMS) of the EMG trace was >0.01 mV were excluded from the MEP analyses. The first 80 ms of the EMG sweep was used to calculate the RMS power. Mean MEP amplitudes were computed for each condition for each participant. These values were then normalized by dividing them by the mean active baseline MEPs (pre-GO TMS pulse). Across participants, an average number of 29 GO MEPs per TMS pulse latency and per block type (STOP and STOP-CHANGE) were included in further analysis. In signal trials, there were, on average, 52 resulting MEPs per TMS pulse latency and block type.

Statistical analysis. To investigate differences between stopping- and changing-condition measurements, we used two-tail paired t tests. Pearson's correlations were also performed across participants to assess the relationship between behavioral and neurophysiological measurements. When multiple tests were used, a false-discovery rate (FDR) correction (Benjamini et al., 2006) was applied to p values to account for Type I error inflation. For significant differences, a 95% confidence interval (CI_{95}) and Cohen's d effect size were reported. For nonsignificant results, we reported the Bayes factor evidence for the null hypothesis (BF_{01}; Krekelberg, 2023).

Data availability. The data files, as well as the scripts for running the task and analyzing the data can be found on the Open Science Framework at https://osf.io/8kmuv/.

Results

Behavior

The main behavioral and CSE results for Experiment 1 are presented in Figure 2. Values for p(resp|signal) did not differ between STOP and STOP-CHANGE tasks (paired t test, $t_{(23)} = 1.01$; $p = 0.32$; $BF_{01} = 2.94$) and were in both cases not significantly different from 0.50 (STOP, $t_{(23)} = 0.16$; $p = 0.87$; $BF_{01} = 4.60$; STOP-CHANGE, $t_{(23)} = 0.85$; $p = 0.40$; $BF_{01} = 3.36$). In addition, US-RT and UC-RT were significantly shorter than GO_{STOP}-RT (paired t test, $t_{(23)} = 6.74$; $p < 0.001$; CI_{95}[37, 70 ms]; Cohen's $d = 0.75$) and $GO_{STOP\text{-}CHANGE}$ RT ($t_{(23)} = 7.81$; $p < 0.001$; CI_{95}[37 ms, 63 ms]; $d = 0.77$), respectively. These manipulation checks verified that the assumptions of the race model held (Verbruggen et al., 2019) and permitted reliable $SSRT_{STOP}$ and $SSRT_{STOP\text{-}CHANGE}$ estimations.

The average participants' GO trials accuracy was 0.98 (SD = 0.03) in STOP blocks and 0.97 (SD = 0.02) in CHANGE blocks. The difference between GO_{STOP}-RT ($M = 537$ ms; SD = 61 ms) and $GO_{STOP\text{-}CHANGE}$ RT ($M = 550$ ms; SD = 67 ms) was not significant ($t_{(23)} = 2.00$; $p = 0.057$; $BF_{01} = 0.85$), and the two values were highly correlated across participants (Pearson's $r_{(22)} = 0.89$; $p < 0.001$; CI_{95}[0.76, 0.95]).

The behavioral inhibition latencies, $SSRT_{STOP}$ ($M = 275$ ms; SD = 36 ms) and $SSRT_{STOP\text{-}CHANGE}$ ($M = 270$ ms; SD = 50 ms), did not differ significantly ($t_{(23)} = 0.98$; $p = 0.33$; $BF_{01} = 3.01$) and were highly correlated ($r_{(22)} = 0.89$; $p < 0.001$; CI_{95}[0.77, 0.95]), suggesting commonalities in the response cancellation required in STOP and STOP-CHANGE trials. In STOP-CHANGE blocks, the GO2-RT ($M = 518$ ms; SD = 60 ms) was tendentially (no statistical significance) shorter than GO_{CHANGE}-RT ($t_{(22)} = 2.03$; $p = 0.05$; CI_{95}[−1 ms, 64 ms]; $d = 0.49$), suggesting that response changing might be faster than its primary initiation. Overall, these results suggest a broad commonality of processing across STOP and STOP-CHANGE blocks.

Nonselective CSE suppression

First, we verified that the baseline MEP amplitude did not differ between STOP and STOP-CHANGE blocks, which it did not ($t_{(23)} = 1.30$; $p = 0.20$; $BF_{01} = 2.20$). In addition, the GO MEP amplitude did not differ across block type and latencies (all uncorrected $p > 0.68$).

Second, we assessed the significance of the expected nonselective MEP reduction in STOP blocks to replicate previous findings of global CSE suppression in human action-stopping (Badry et al., 2009; Wessel et al., 2022). The MEP amplitude was significantly lower in SS than GO trials at all three latencies (paired t test with FDR correction, 150 ms, $t_{(23)} = 3.16$; $p_{FDR} = 0.006$; CI_{95}[0.04, 0.19]; $d = 0.63$; 175 ms, $t_{(23)} = 3.97$; $p_{FDR} < 0.001$; CI_{95}[0.07, 0.21]; $d = 0.73$; 200 ms, $t_{(23)} = 2.40$; $p_{FDR} = 0.02$; CI_{95}[0.01, 0.11]; $d = 0.58$).

Third, the main hypothesis of Experiment 1 was that nonselective CSE suppression would also occur in STOP-CHANGE trials. The hypothesis was verified, as SC trials MEPs were reduced as compared with GO_{CHANGE} trials (paired t test, 150 ms, $t_{(23)} = 3.28$; $p_{FDR} = 0.005$; CI_{95}[0.05, 0.22]; $d = 0.68$; 175 ms, $t_{(23)} = 4.02$; $p_{FDR} < 0.001$; CI_{95}[0.07, 0.21]; $d = 0.81$; 200 ms, $t_{(23)} = 2.08$; $p_{FDR} = 0.049$; CI_{95}[0.01, 0.16]; $d = 0.46$).

Fourth, to compare the level of nonselective CSE suppression engaged in successful action-stopping and action-changing, we compare SS versus SC trials MEPs. This contrast showed no difference across the three TMS pulse latencies (all uncorrected $p > 0.26$). In addition, SS and SC MEP values were significantly correlated across participants at the three TMS latencies (150 ms, $r_{(22)} = 0.75$; $p_{FDR} < 0.001$; CI_{95}[0.50, 0.89]; 175 ms,

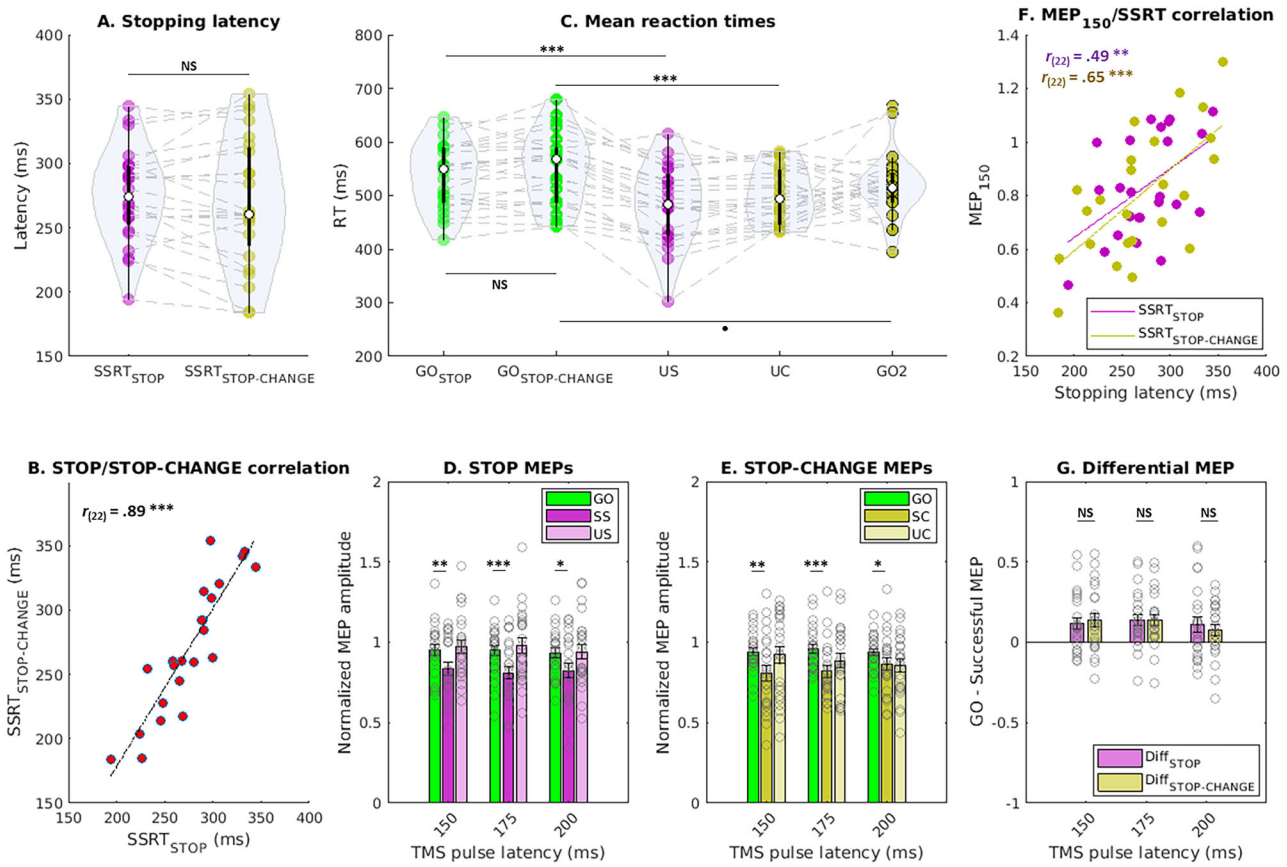

Figure 2. Behavior and CSE results of Experiment 1. ***A,B***, Behavioral response stopping latencies (SSRTs) estimated for action-stopping and action-changing and their correlation across participants. ***C***, Individuals' mean RT in GO, unsuccessful STOP/STOP-CHANGE (US, UC), and successfully changed responses (GO2). ***D,E***, MEP amplitudes in STOP- and STOP-CHANGE-task blocks, respectively. ***F***, MEPs/behavior correlations. ***G***, GO versus successful signal trial MEPs contrast in stopping and changing. •$p = 0.05$; *$p_{FDR} < 0.05$; **$p_{FDR} < 0.01$; ***$p_{FDR} < 0.001$.

$r_{(22)} = 0.76$; $p_{FDR} < 0.001$; $CI_{95}[0.51, 0.89]$; 200 ms, $r_{(22)} = 0.62$; $p_{FDR} = 0.001$; $CI_{95}[0.29, 0.82]$). We further computed for each block type the difference (ΔMEP) between successful STOP-CHANGE and GO trials MEPs. This contrast indicated a similar level of global CSE suppression between the two block type as ΔMEP_{STOP} and $\Delta MEP_{STOP\text{-}CHANGE}$ did not differ (paired t test, 150 ms, $t_{(23)} = 0.53$; $p = 0.60$; $BF_{01} = 4.09$; 175 ms, $t_{(23)} = 0.03$; $p_{FDR} = 0.98$; $BF_{01} = 4.66$; 200 ms, $t_{(23)} = 0.85$; $p = 0.40$; $BF_{01} = 3.36$). Bayes factor indicated moderate evidence for similar suppression levels between stopping and changing.

Fifth, we assessed the behavioral relevance of nonselective CSE suppression at the earliest latency (150 ms). The MEP amplitude in SS and SC trials was significantly correlated to $SSRT_{STOP}$ ($r_{(22)} = 0.49$; $p = 0.01$; $CI_{95}[0.11, 0.75]$) and $SSRT_{STOP\text{-}CHANGE}$ ($r_{(22)} = 0.65$; $p < 0.001$; $CI_{95}[0.33, 0.83]$), respectively, reflecting that larger CSE suppression was associated with faster response cancelation in both stopping and changing tasks.

Experiments 2 and 3

Materials and Method

Hypotheses. Experiment 1 showed that nonselective CSE suppression reflects a global "pause" stage that is commonly triggered in action-stopping and action-changing. Experiments 2 and 3 investigated the other proposed neurophysiological signatures of inhibitory control. Based on PTC predictions, we anticipated that frontocentral EEG β-bursts dynamics and partial EMG responses show an increase after STOP and STOP-CHANGE signals, as compared with GO signals, with no difference between stopping and changing. In addition, we hypothesized that the amplitude of "cancel" inhibition-stage signatures, including frontocentral P3 ERP and θ power (Diesburg and Wessel, 2021; Messel et al., 2021), scale with the required action revision (see below).

For the EEG and EMG investigations, we used a task in which STOP and CHANGE trials were intermixed within task blocks. Indeed, previous works have suggested that the block design modulates the $SSRT_{STOP}$ versus $SSRT_{STOP\text{-}CHANGE}$ difference (Boecker et al., 2013). After showing similar $SSRT_{STOP}$ and $SSRT_{STOP\text{-}CHANGE}$ in a between-block design (Experiment 1), Experiments 2 and 3 compared these measures in a within-block design. Furthermore, beyond the action-stopping versus action-changing comparison, we investigated whether EEG signatures of inhibitory control would be affected by modulating the amount of action change. Therefore, we included two types of STOP-CHANGE signals. In STOP-CHANGE-side (CS) trials, participants had to change one response dimension, similar to Experiment 1 (see below). In STOP-CHANGE-side-and-finger (CSF) trials, participants had to change two dimensions of the response (see below). In Experiment 2, the 1/3 of trials in which a signal was presented were divided by the three signal types: 1/9 STOP, 1/9 CS, and 1/9 CSF. Then, to ensure that our results were not led by the higher probability of CHANGE trials (2/9 for CS + CSF count) compared with STOP trials (1/9), we aimed to replicate our findings in a separate experiment. That experiment used the exact same task design in Experiment 3 but included a

modification of these probabilities. The 1/3 of signal trials were divided into half STOP trials (1/6) and half STOP-CHANGE trials (1/12 CS and 1/12 CSF). Empirically, these probabilities did not influence any of the results in a significant fashion. We will therefore present data from the combined sample ($N = 52$) to achieve the highest amount of statistical power and fidelity.

Participants. Thirty healthy individuals (16 females; mean age 19.4 years, SD = 1.2) participated in Experiment 2 and twenty-two (16 females, mean age 21.6 years, SD = 4.3) in Experiment 3, respectively, in exchange for course credit or an hourly payment of $15. All were right-handed and had normal or corrected-to-normal vision. None of the participants reported a history of psychiatric or neurological disorders. The experiments were performed with the informed consent of all participants, and procedures were approved by the local IRB (IRB Number 201612707) and conducted in accordance with the Declaration of Helsinki.

Experimental task. The behavioral task was presented on a Linux desktop computer using on Matlab 2017b (The MathWorks) and the Psychophysics Toolbox (Brainard, 1997). The task design is depicted in Figure 3.

The main GO task was a four-choice RT task. In each trial, after four white squares were presented for a random duration ranging from 500 to 750 ms, one of the squares turned green, representing the GO stimulus. Participants were instructed to respond quickly and accurately to the GO stimulus by pressing the corresponding key on the response device, a keyboard with four keys colored in white to match the four potential GO stimuli spatially. Responses were made with the right/left index finger or thumb. In a randomly chosen 1/3 of the trials, the initial green square (GO) turned into a STOP or STOP-CHANGE signal after the SSD. If the green square turned blue, this was a STOP signal, instructing participants to try to cancel the GO response. If the initial green square turned blue while another white square turned green at the same time, this was a STOP-CHANGE signal, instructing participant to try to cancel the initial GO response and, instead, press the key corresponding to the new green stimulus. The STOP-CHANGE signal always engaged a switch in the response side (e.g., left to right) but could either engage an additional finger switch (left index finger to right thumb) or no finger switch (left index finger to right index finger), thus implying to modify two versus one dimensions of the response. Therefore, three signal types could have been displayed after the initial GO stimulus: STOP signal, CS signal (STOP-CHANGE-side), and CSF signal (STOP-CHANGE-side-and-finger). Specific to each signal type and each finger, the SSD incremental adjustment was similar to Experiment 1 to achieve a probability of responding p(resp|signal) of ~0.50 in signal trials. Trials were categorized as GO trials, SS/SCS/SCSF trials (successful stopping and changing trials), or US/UCS/UCSF (unsuccessful stopping and changing trials). Erroneous responses (i.e., pressing another key than the cued GO or CHANGE responses) were excluded (<1% of the data). If the RT to the GO stimulus or STOP-CHANGE signal was above 1,000 ms, the feedback "Too slow!" was displayed on the screen for a 500 ms duration. Overall, the duration between two subsequent GO stimuli was 3,000 ms. The participants performed 1,008 trials through 14 blocks of 72 trials (48 GO trials + 24 signal trials). Each block started with three consecutive GO trials, and written and verbal feedback was provided after each block as described in Experiment 1. Before the actual task, four practice blocks of 24 trials each were performed: one GO-only

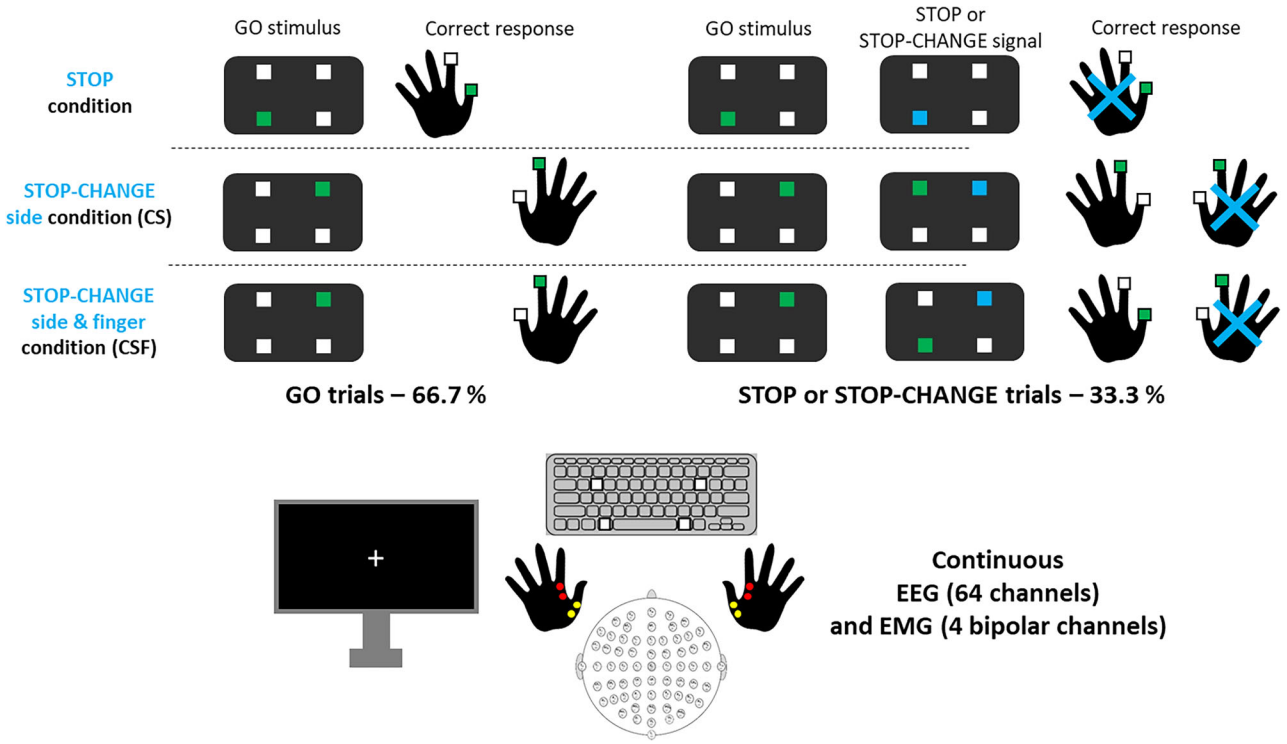

Figure 3. Task diagram of Experiment 2 and 3. Time course of the behavioral task. Following the presentation of the green GO target, the target changed to blue in a minority of trials (33.3%). These signaled the participant to try to stop their initial response (STOP signal) or stop the initial response for changing it with the newly instructed response: another green target (STOP-CHANGE-side or STOP-CHANGE-side-and-finger signal). Setup additionally involved a scalp EEG recording and EMG recordings of first-dorsal interosseous muscles for index fingers (red) and abductor pollicis brevis muscles for thumbs (yellow).

block, one GO + STOP block, one GO + STOP-CHANGE block, and one intermixed block. This practice was repeated if the p(resp|signal) was outside the 0.40–0.60 range. Green and blue color correspondence to GO stimuli and STOP/STOP-CHANGE signals was randomized across participants.

EEG and EMG recording. EEG was acquired using a 64-channel active electrode cap connected to an ActiCHamp amplifier (Brain Products). The ground and reference electrodes were placed at AFz and Pz, respectively. EMG was recorded from the first-dorsal interosseous muscles for index fingers and abductor pollicis brevis muscles for thumbs following previous recommendations (Coxon et al., 2006; Raud et al., 2022). For each, two electrodes were placed on the belly and tendon of the muscle. Ground electrodes were placed on the distal end of each hand's ulna (for indexes) and radius (for thumbs). The EMG electrodes were connected to the EEG system using two auxiliary channels (via BIP2AUX adaptor cables). Thus, there were 68 total recording channels. All channels were sampled at a rate of 2,500 Hz. To minimize task-unrelated EMG activity, the participants were instructed only to move their fingers when necessary and to keep both hands otherwise relaxed and pronated on the desk.

EEG and EMG preprocessing. Custom MATLAB scripts, including EEGLAB (Delorme and Makeig, 2004) toolbox functions, were used to preprocess the EEG and EMG data. Both EEG and EMG data were bandpass filtered (EEG, 0.1–50 Hz; EMG, 20–250 Hz) and downsampled to a rate of 500Hz. The continuous EEG data were visually inspected to identify nonstereotypical artifacts. Segments with nonstereotypical EEG artifacts were removed from the EEG and EMG data. EEG and EMG data were epoched relative to the onsets of GO stimuli (−500 to 2,000 ms). Missed and incorrect GO trials were excluded from all analyses. The EEG data were re-referenced to the common average. Independent component analysis (Infomax ICA; Bell and Sejnowski, 1995) was applied to the cleaned EEG data (concatenation of the EEG epochs) to identify neural components contributing to the observed scalp data. Using the ICLABEL classifier (Pion-Tonachini et al., 2019), the components associated with an above 0.90 probability to be artifactual were removed from the EEG data structure, thus removing their contributions to the observed EEG. Rejection was systematically checked by visual inspection of component properties (time series, spectra, topography) according to ICLABEL guidelines. The EMG data were then converted to RMS power using a sliding window of 10 sample points and baseline-corrected by dividing the entire epoch by the mean of the 200 ms prestimulus EMG. The resulting data were then standardized for each finger across all types of trials and sample points using the *z*-transform. After EMG data preprocessing, the analysis focused on the to-be-stopped and to-be-revised actions. In each condition (GO, STOP, STOP-CHANGE), the EMG trace of the first instructed response has been included in the analysis.

Behavioral analysis. Similar to Experiment 1, we computed mean participants' RTs: GO-RT (GO trials), US-RT/UCS-RT/UCSF-RT (unsuccessful STOP/STOP-CHANGE trials), and $GO2_{CS}$-RT/$GO2_{CSF}$-RT (new response for successful STOP-CHANGE trials). The behavioral inhibition latency was also estimated according to the signal type: $SSRT_{STOP}$/$SSRT_{CS}$/$SSRT_{CSF}$.

EMG data analysis. As a manipulation check, we examined whether the EMG data accurately captured the participant's motor responses on GO trials. Single-trial GO-RTs were correlated to EMG peak latencies within each EMG channel (Pearson's *r*). The EMG peak was computed as the maximal value within the RT window. For those correlations, trials in which Cook's *D* exceeded 4/*N*, with *N* the number of channel's data points, were deemed statistical outliers and excluded from further analysis. Then, channels with a *r* value lower than 0.5 were also excluded, due to potential disconnections of the electrodes during the experiment. Participants with more than one rejected channel were excluded from the analysis.

For each condition, the trial-to-trial EMG peak was identified, as explained above. This procedure was applied for trials with a behavioral response (GO, US, UCS and UCSF trials). For trials with no response to the primary target (SS, SCS, and SCSF trials), we aligned with previous studies to identify partial EMG (prEMG) responses (Jana et al., 2020; Tatz et al., 2021; Raud et al., 2022). Within a window corresponding to the maximal RT of each participant, an EMG burst was identified in a trial if any data point exceeded a threshold of 1.2 (in standard deviation units, taking into account all trials; Raud et al., 2020, 2022). The peak latency was defined as the time point of the highest amplitude in a trial. Lastly, peak latencies of the EMG were recalculated relative to the stop signal onset by subtracting the trial SSD.

EEG data analysis. Previous studies have shown that β-burst dynamics convey inhibitory commands along corticosubcortical networks, from subthalamic nucleus (STN) to M1 (Cagnan et al., 2019; Diesburg et al., 2021) and from frontocentral sites to sensorimotor sites (Wessel, 2020; Choo et al., 2022). We thus computed frontocentral β-bursts as an index of early cortical inhibitory mechanisms (Hannah et al., 2020; Jana et al., 2020; Tatz et al., 2023). The FCz electrode's data were convolved with a complex Morlet wavelet of the form as follows:

$$w(t,f) = A\exp\left(-\frac{t^2}{2\sigma_t^2}\right)\exp\left(2i\pi ft\right),$$

with $\sigma = \frac{m}{2\pi f}$, $A = \frac{1}{\sigma_t}\sqrt{2\pi}$ and m (cycles) ranging from five to nine across the 15 evenly spaced frequencies spanning the β-band (15–29 Hz). Time–frequency power estimates were extracted by calculating the squared magnitude of the complex wavelet-convolved data. Individual β-bursts were identified in the trial-by-trial β-band time–frequency power matrix based on power exceeding a cutoff of two times the median power of the entire time–frequency power matrix for that electrode. Individual's β-burst rates were computed for each condition based on a 50-ms-length sliding window (Choo et al., 2022; Tatz et al., 2023). Time point-wise, the number of bursts across trials was summed within the window and divided by the number of trials. β-Burst volume was computed for each burst through numerical integration of the suprathreshold data points (Enz et al., 2021). A similar sliding-window averaging resulted in a single vector reflecting the β-burst volume time dynamic for each condition and each participant. These β-burst rate and volume time series were then relocked for each condition to the onset of the STOP/STOP-CHANGE signal or the match GO latency (GO stimulus onset + average participant's SSD). Individuals' vectors were normalized by dividing the values by the average of the −200 to 0 ms baseline period. Then, we computed individuals' average normalized β-burst rate and volume within each participant's SSRT window.

Second, EEG correlates of action-stopping are classically observed at later latencies with stop signal-related frontocentral

P3 wave and θ power increase (Huster et al., 2013; Wessel and Aron, 2015; Dykstra et al., 2020; Messel et al., 2021; Waller et al., 2021). According to extant theoretical proposals, both are thought to index a later selective stage of the inhibitory control that specifies the need to cancel the response (Diesburg and Wessel, 2021; Tatz et al., 2021; Waller et al., 2021). Individuals' frontocentral ERPs were obtained for each condition by averaging FCz site EEG data across trials. To compute θ power, we bandpass filtered FCz data in the 4–8 Hz frequency range. The filtered time series were then translated into complex space using the Hilbert transform (as implemented in the MATLAB *hilbert* function). θ power was then extracted by computing the square of the absolute of the complex output of the Hilbert transform. Individuals' ERPs and θ power were re-epoched into a −200 to 800 ms surrounding the STOP/STOP-CHANGE signal onset (or match GO), and we subtracted a baseline defined as the average signal in the −200 to 0 ms window. P3 and θ amplitudes were defined as the maximal value of the ERP and power time series. Following Wessel and Aron (2015), the P3 onset was defined as the earliest time point at which a statistically significant deviation between STOP/STOP-CHANGE and matched GO trials ERPs could be detected in a given participant. For this, *t* tests were performed across single-trial EEG. Working back over data samples from the P3 peak, the earliest sample point at which the STOP-CHANGE ERP significantly exceeded the GO ERP was selected as the participant's P3 onset. Individuals' ERP peaks and onsets were successfully computed in all task conditions for most of the participants. When an individual's value was unsuccessfully captured for a given condition, this participant was removed from the statistical comparisons involving this condition. Therefore, degrees of freedom ranged from 40 to 50 for the statistical comparisons we performed.

Third, we completed our comparative analysis of the neurophysiological dynamic of action-stopping versus action-changing by investigating at which time point a multivariate pattern analysis (MVPA) classifier applied to the whole-scalp EEG would be able to distinguish between the conditions of interest above chance. MVPA analyses were performed using the ADAM toolbox (Fahrenfort et al., 2018) on the preprocessed 64 channels' data. We used leave-one-out cross–validation in which a linear discriminant analysis classifier was trained on all trials, but one, and tested on the remaining trial that was not part of the training set. This validation was implemented in a sample point-wise fashion, in which training and testing were done at each sample point following the STOP/CS/CSF signal. Classifier performance was measured as the area under the receiver operating characteristics curve (AUC) (Wickens, 2002), which quantified the total AUC when the cumulative true positive rate (probability of correct classification) was plotted against the false-positive rate (probability of incorrect classification) for each decoding problem between the conditions of interest. Time series of AUC values were obtained for each pair of conditions and each participant. To identify time points during which classification performance was significantly above chance, we compared each AUC value against chance-level performance (0.5) using one-sample *t* tests, which was corrected for multiple comparisons using cluster-based permutation testing (10,000 iterations; cluster $p = 0.00001$; individual sample point $a = 0.0001$; Maris and Oostenveld, 2007).

Results

The results of Experiments 2 and 3 converged toward a highly similar pattern. Therefore, the analyses presented below were performed on the two experiments' data altogether ($N = 52$) to increase statistical power. To ensure that Experiment 2 and 3 results followed a similar pattern, we assessed the null difference between the two experiments in the main behavioral measures: GO-RT ($t_{(49)} = 0.26$; $p_{FDR} = 0.80$; $BF_{01} = 3.46$), $SSRT_{STOP}$ ($t_{(49)} = 1.79$; $p_{FDR} = 0.32$; $BF_{01} = 1.00$), $SSRT_{CS}$ ($t_{(49)} = 0.52$; $p_{FDR} = 0.80$; $BF_{01} = 3.18$), and $SSRT_{CSF}$ ($t_{(49)} = 0.49$; $p_{FDR} = 0.80$; $BF_{01} = 3.22$).

Behavior

The main behavioral results of Experiments 2 and 3 are depicted in Figure 4. One participant was rejected because of an outlier $SSRT_{STOP}$ value ($< M \pm 3$ SD). The final sample for the behavioral analysis was $N = 51$. The average participants' GO trials accuracy was 0.98 (SD = 0.02). In STOP trials, p(resp|signal) ($M = 0.46$; SD = 0.05) was significantly lower than CS trials ($M = 0.51$; SD = 0.02; paired *t* test with FDR correction, $t_{(50)} = 7.01$; $p_{FDR} < 0.001$; CI_{95}[0.03, 0.06]; Cohen's $d = 1.01$) and CSF trials ($M = 0.51$; SD = 0.02; $t_{(50)} = 6.62$; $p_{FDR} < 0.001$; CI_{95}[0.03, 0.06]; $d = 0.99$). CS and CSF conditions did not differ ($t_{(50)} = 0.32$; $p_{FDR} = 0.75$; $BF_{01} = 6.26$). These results indicate a higher successful cancellation rate of the initial response in action-changing compared with action-stopping (despite adaptive tracking being used for both).

Verifying race model assumptions (Verbruggen et al., 2019), GO-RT ($M = 418$ ms; SD = 57 ms) was significantly longer than US-RT ($M = 386$ ms; SD = 46 ms; paired *t* test, $t_{(50)} = 9.87$; $p_{FDR} < 0.001$; CI_{95}[26 ms, 39 ms]; $d = 0.60$), UCS-RT ($M = 396$ ms; SD = 51 ms; $t_{(50)} = 6.25$; $p_{FDR} < 0.001$; CI_{95}[15 ms, 30 ms]; $d = 0.41$), and UCSF-RT ($M = 391$ ms, SD = 48 ms; $t_{(50)} = 8.22$, $p_{FDR} < 0.001$, CI_{95}[20 ms, 34 ms], $d = 0.50$). These manipulation checks verified that the assumptions of the race model held and permitted reliable $SSRT_{STOP}$ and $SSRT_{CHANGE}$ estimations.

Suggesting a faster initial-response cancellation in action-changing than action-stopping, $SSRT_{STOP}$ ($M = 226$ ms; SD = 25 ms) was significantly longer than $SSRT_{CS}$ ($M = 161$ ms; SD = 43 ms; $t_{(50)} = 11.60$; $p_{FDR} < 0.001$; CI_{95}[54 ms, 76 ms]; $d = 1.35$) and $SSRT_{CSF}$ ($M = 163$ ms; SD = 41 ms; $t_{(50)} = 12.00$; $p_{FDR} < 0.001$; CI_{95}[53 ms, 74 ms]; $d = 1.36$), while $SSRT_{CS}$ and $SSRT_{CSF}$ did not differ ($t_{(50)} = 0.29$; $p_{FDR} = 0.77$; $BF_{01} = 8.16$). A moderate correlation was found for $SSRT_{STOP}$/$SSRT_{CS}$ (Pearson's $r_{(49)} = 0.41$; $p_{FDR} = 0.003$; CI_{95}[0.15, 0.61]) and $SSRT_{STOP}$/$SSRT_{CSF}$ ($r_{(49)} = 0.44$; $p_{FDR} = 0.02$; CI_{95}[0.19, 0.64]), while the $SSRT_{CS}$/$SSRT_{CSF}$ correlation was stronger ($r_{(49)} = 0.63$; $p_{FDR} < 0.001$; CI_{95}[0.43, 0.77]).

Similar to Experiment 1, response changing was faster than its primary initiation. GO-RT ($M = 418$ ms; SD = 57 ms) was longer than $GO2_{CS}$-RT ($M = 348$ ms; SD = 90; $t_{(50)} = 6.70$; $p_{FDR} < 0.001$; CI_{95}[50 ms, 92 ms]; $d = 0.85$) and $GO2_{CSF}$-RT ($M = 332$ ms; SD = 94 ms; $t_{(50)} = 7.90$; $p_{FDR} < 0.001$; CI_{95}[64 ms, 108 ms]; $d = 0.97$). Interestingly, $GO2_{CS}$-RT was longer than $GO2_{CSF}$-RT ($t_{(50)} = 3.31$; $p_{FDR} = 0.002$; CI_{95}[6 ms, 25 ms]; $d = 0.17$).

prEMG

Grand-average EMG waveforms and analysis results are depicted in Figure 5 for Experiments 2 and 3. In addition to the participant excluded based on behavior (see above), six participants were excluded due to noisy EMG data (see Materials and Methods for detailed criteria), resulting in a final sample of $N = 45$ analyzed datasets. Our manipulation-check procedure showed that EMG accurately captured the participants' motor responses. The single-trial correlation between GO-RT and EMG peak latency was high for every channel (Pearson's *r*, $M = 0.93$; SD = 0.07). Among 180 recorded channels (45 participants × 4 fingers), 8 were rejected, and an average 7% of trials were rejected

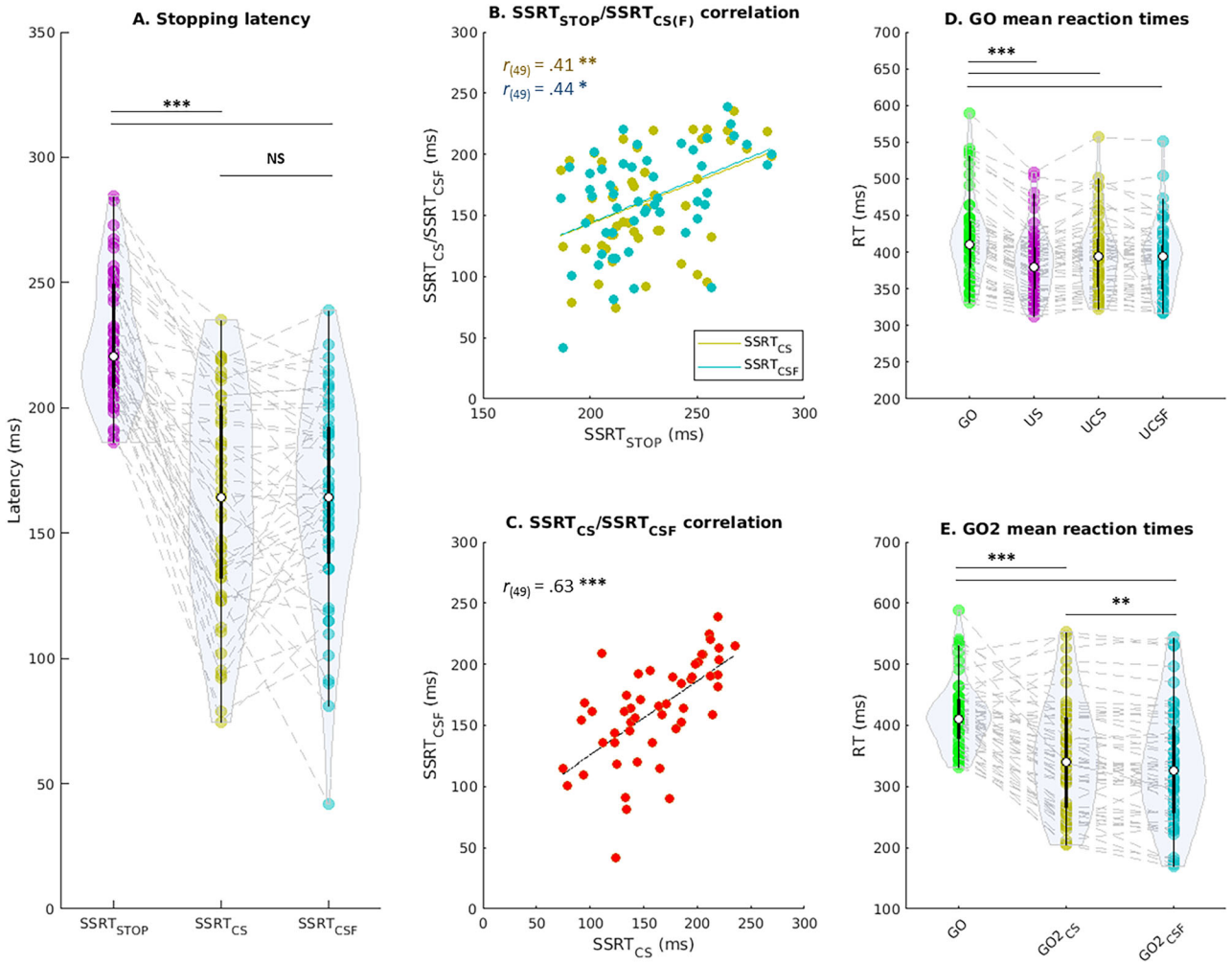

Figure 4. Behavior results of Experiments 2 and 3. ***A***, Behavioral initial-response inhibition latencies (SSRTs) estimated for action-stopping and action-changing. ***B***, Correlations between STOP and STOP-CHANGE SSRT estimates across participants. ***C***, Correlation between change-side and change-side-and-finger SSRT estimates across participants. ***D***, Individuals' mean RT in GO and unsuccessful STOP/STOP-CHANGE (US, UCS, UCSF) responses. ***E***, Individuals' mean RT in successfully changed responses ($GO2_{CS}$, $GO2_{CSF}$). *$p_{FDR} < 0.05$; **$p_{FDR} < 0.01$; ***$p_{FDR} < 0.001$.

in the retained channels. The proportion of prEMG identified across successfully aborted initial responses was similar to previous investigations with stop-signal tasks (see Raud et al., 2022, for a meta-analysis). This proportion in SS trials ($M = 0.42$) was lower than SCS ($M = 0.55$; $t_{(44)} = 6.46$; $p_{FDR} < 0.001$; CI_{95}[0.09, 0.16]; $d = 0.68$) and SCSF trials ($M = 0.54$; $t_{(44)} = 6.09$; $p_{FDR} < 0.001$; CI_{95}[0.08, 0.16]; $d = 0.63$), while it did not differ between SCS and SCSF trials ($t_{(44)} = 0.77$; $p = 0.44$; $BF_{01} = 4.66$).

Averaged waveforms (Fig. 5) show that successfully aborted initial responses in SS, SCS, and SCSF trials were associated with an EMG activation that was present to a lower extent than in response trials (GO, US, UCS, USF). In successfully aborted response, the amplitude of the prEMG (i.e., EMG activity that escaped inhibition) scaled from SS to SCS to SCSF. Indeed, prEMG peak amplitude was significantly lower in SS than SCS ($t_{(44)} = 5.02$; $p_{FDR} < 0.001$; CI_{95}[0.77, 1.80 (z)]; $d = 0.68$) and SCSF trials ($t_{(44)} = 5.53$; $p_{FDR} < 0.001$; CI_{95}[1.48, 3.17 (z)]; $d = 0.95$), while SCS prEMG amplitude was also lower than SCSF trials ($t_{(44)} = 3.81$; $p_{FDR} < 0.001$; CI_{95}[0.49, 1.59 (z)]; $d = 0.44$). Our results clearly show the presence of a prEMG in successful action-stopping, in line with previous studies (Raud et al., 2022). In addition, our analysis shows a scaling dynamic of the prEMG across our conditions, indicating that the initial-response prEMG amplitude was higher in action-changing than action-stopping.

The same analysis was performed for prEMG peak latency, showing that prEMG peak occurred earlier in CHANGE than STOP trials. Indeed, prEMG peak latency was later in SS ($M = 230$ ms; SD =65 ms) than SCS ($M = 165$ ms; SD = 62 ms; $t_{(44)} = 6.63$; $p_{FDR} < 0.001$; CI_{95}[45 ms, 85 ms]; $d = 0.91$) and SCSF trials ($M = 143$ ms; SD = 50 ms; $t_{(44)} = 10.51$; $p_{FDR} < 0.001$; CI_{95}[72 ms, 106 ms]; $d = 1.20$). SCS and SCSF prEMG peak latencies also differ ($t_{(44)} = 4.44$; $p_{FDR} < 0.001$; CI_{95}[10 ms, 26 ms]; $d = 0.39$). These analyses showed a scaling dynamic across our conditions, the aborted initial-response prEMG peak being earlier when the amount of required response revision was higher.

EEG

STOP/STOP-CHANGE signals induced a frontocentral β-burst dynamics modulation, especially visible as a β-burst volume increase (Fig. 6). SSRT-window analysis revealed no significant modulation of the β-burst rate between STOP/STOP-CHANGE and match GO trials ($p_{FDR} > 0.05$) but showed an increase of β-burst volume in SS ($t_{(49)} = 2.35$; $p_{FDR} = 0.02$; CI_{95}[0.04, 0.51]; $d = 0.40$), SCS ($t_{(49)} = 2.17$; $p_{FDR} = 0.03$; CI_{95}[0.01, 0.31]; $d = 0.35$) and SCSF trials ($t_{(49)} = 2.06$; $p_{FDR} = 0.04$; CI_{95}[0.01, 0.44]; $d = 0.35$), as compared with match GO trials. The SSRT-window β–burst rate and volume did not

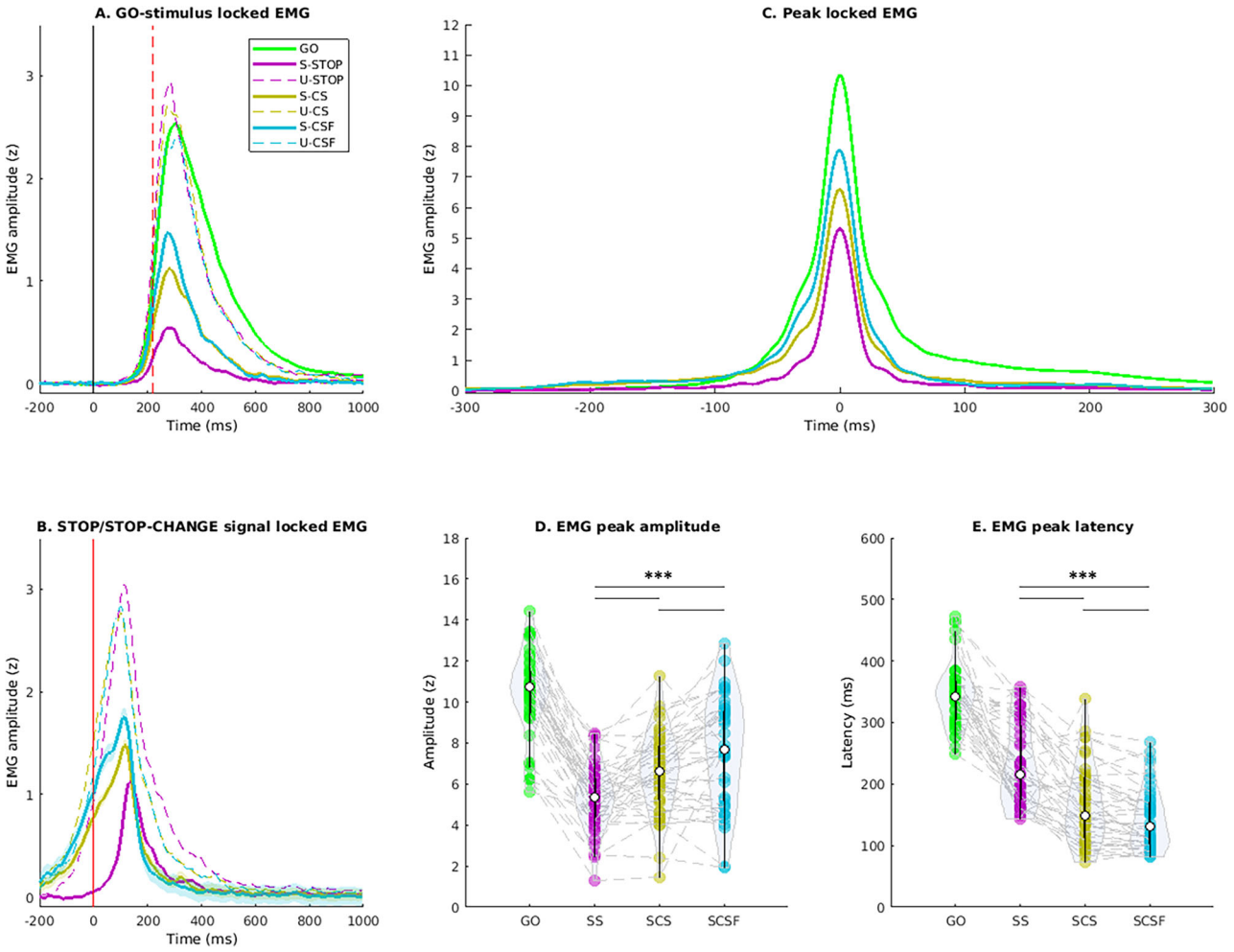

Figure 5. prEMG results of Experiment 2 and 3. ***A***, GO stimulus locked grand-average EMG waveforms of the response triggered by the primary target (the red line is the stop-signal occurrence time). ***B***, STOP/STOP-CHANGE signal locked grand-average EMG waveforms. ***C***, Peak locked grand-average EMG waveforms. ***D***, Individuals' prEMG peak amplitude (and latency, panel ***E***, for successfully aborted responses in SS, SCS, and SCSF trials. *$p_{FDR} < 0.05$; **$p_{FDR} < 0.01$; ***$p_{FDR} < 0.001$.

show any significant difference across $SSRT_{STOP}$, $SSRT_{CS}$, and $SSRT_{CSF}$ ($p_{FDR} > 0.05$; $BF_{01} > 3$). Overall, the β-burst volume showed an increase during SSRT which was identical across conditions.

ERPs showed a clear P3 wave evoked by the STOP/STOP-CHANGE signal with a frontocentral topography (Fig. 7). In line with the visual inspection of the ERPs, the P3 onset analysis confirmed that the P3 wave was engaged in action-stopping and action-changing as its onset was earlier in successfully compared with unsuccessfully canceled responses. Indeed, the SS P3 onset ($M = 247$ ms; SD = 43 ms) was earlier than US ($M = 274$ ms; SD = 40 ms; paired t test, $t_{(40)} = 3.67$; $p_{FDR} < 0.001$; CI_{95}[12 ms, 41 ms]; $d = 0.62$); this was also the case for SCS ($M = 216$ ms; SD = 54 ms) compared with USC ($M = 250$ ms; SD = 39 ms; $t_{(41)} = 3.71$; $p_{FDR} < 0.001$; CI_{95}[14 ms, 47 ms]; $d = 0.67$) and SCSF ($M = 218$ ms; SD = 37 ms) compared with UCSF ($M = 239$ ms; SD = 38 ms; $t_{(44)} = 5.25$; $p_{FDR} < 0.001$; CI_{95}[13 ms, 30 ms]; $d = 0.52$). In line with our PTC model-based hypothesis, we observed that P3 amplitude scaled with the engaged action revision. First, the P3 amplitude was higher in successful changing conditions, compared with stopping. Second, the P3 amplitude increased when adding a response dimension to revise (change-side-and-finger vs change-side). Indeed, the P3 amplitude was lower in SS than SCS (paired t test, $t_{(40)} = 2.29$; $p_{FDR} = 0.03$; CI_{95}[0.09, 1.41]; $d = 0.17$) and SCSF trials ($t_{(40)} = 3.12$; $p_{FDR} = 0.01$; CI_{95}[0.43, 2.03]; $d = 0.26$). Importantly, P3 was also larger in SCSF compared with SCS ($t_{(42)} = 2.21$; $p_{FDR} = 0.03$; CI_{95}[0.06, 1.00]; $d = 0.10$), meaning that an additional response dimension to revise was associated with larger P3. We also computed an additive model to compare STOP-CHANGE P3 peak versus [GO P3 + SS P3] peak. STOP-CHANGE P3 was still significantly higher for both SCS and SCSF conditions ($p_{FDR} < 0.05$). Together, these results coherently indicate that frontocentral P3 wave scaled with the amount of engaged response revision, in a SS→SCS→SCSF order. Accordingly, θ power was increased post-STOP/STOP-CHANGE signal and scaled with the amount of response update. Indeed, SS θ power amplitude was lower than SCS ($t_{(49)} = 2.59$; $p_{FDR} = 0.02$; CI_{95}[1.71, 13.58]; $d = 0.23$) and SCSF trials ($t_{(49)} = 2.79$; $p_{FDR} = 0.02$; CI_{95}[2.01, 12.36]; $d = 0.23$). There was no significant difference between SCS and SCSF conditions ($t_{(49)} = 0.19$; $p_{FDR} = 0.85$; $BF_{01} = 7.50$). Aligning with the P3 dynamic, these results showed that the θ power increase induced by a STOP-CHANGE signal was larger than a STOP signal. However, the SCS versus SCSF difference being unique to P3 might suggest that θ more generically reflects the larger cognitive control required in changing than stopping. In contrast, the finer P3 scaling according to the required response revision would reflect the actual "retuning" of the motor response.

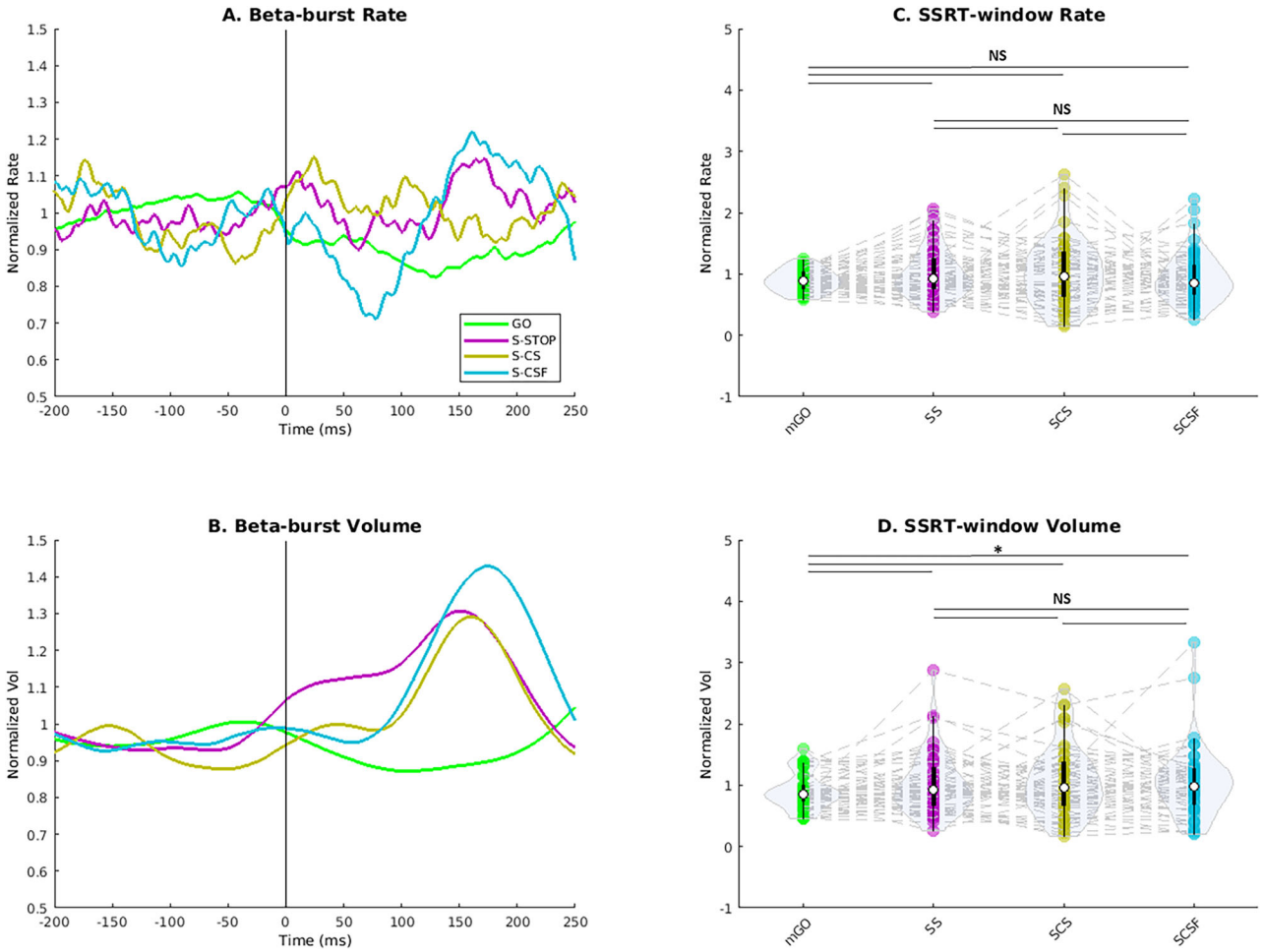

Figure 6. β-Bursts results of Experiment 2 and 3. ***A,B***, The grand-average β–burst rate and volume computed at the FCz site and locked to the STOP/STOP-CHANGE signal. ***C,D***, individual's averaged β-burst rate and volume within SSRT windows. *$p_{FDR} < 0.05$; **$p_{FDR} < 0.01$; ***$p_{FDR} < 0.001$.

Finally, the whole-scalp EEG MVPA decoding significantly decoded STOP and STOP-CHANGE trials starting 189 ms for SCS and 132 ms for SCSF. Maximum classification performances reached 0.68 (SS vs SCS) and 0.67 (SS vs SCSF). The MVPA procedure also succeeded in significantly distinguishing SCS and SCSF conditions starting at 311 ms (maximum performance of 0.58), i.e., the exact time range of the frontocentral P3. These results suggest that STOP and CHANGE conditions started to engage unique EEG activity in an early postsignal window compatible with the late edge of the proposed "pause" inhibitory stage. STOP-CHANGE conditions began to differ, depending on the number of response dimensions (side vs side-and-finger), in a later window compatible with the assumed "cancel"/"retune" timeline.

Discussion

Past work on action-stopping has identified several candidate signatures of inhibitory control. However, they have been hard to reconcile under a joint framework, owing largely to their timing differences and debated functional significance. Evaluating these signatures altogether for the first time, we successfully disentangle their functional properties across multiple action-revision conditions. Accounting for common and unique neurophysiological dynamics, our results support a "pause-then-retune" conceptualization of human action revision in line with two-stage models of action-stopping (Schmidt and Berke, 2017; Diesburg and Wessel, 2021). Early signatures (nonselective CSE suppression and β-burst volume increase) were common to stopping and changing, in line with a shared "pause"-stage inhibition processing. In contrast, later frontocentral θ power was larger for changing than stopping, and P3 scaled with the amount of response revision, in line with the proposal that these signatures reflect a separate "retuning" stage, which is sensitive to the exact demands of the task.

Our results have several notable features. First, the early nonselective CSE suppression was present in both action-stopping and action-changing. This nonselective CSE suppression has been causally associated with the STN in action-stopping based on TMS/DBS combination (Wessel et al., 2022). Therefore, our result is congruent with previous findings from fMRI (Kenner et al., 2010) and STN–DBS in Parkinson's disease (van den Wildenberg et al., 2017, 2021) supporting the engagement of the STN-mediated hyperdirect pathway in both action-stopping and action-changing. Similar early CSE suppression corroborated our prediction that broad inhibition is commonly triggered by a "pause" process in the two situations and rejects the alternative view (Logan and Burkell, 1986; De Jong et al., 1995; Krämer et al., 2011) of inhibition being mainly implemented by "selectively preventing central outflow of motor commands" in action-changing context (De Jong et al., 1995). Besides, increases in SSRT-window β–burst volume did not differ across action-

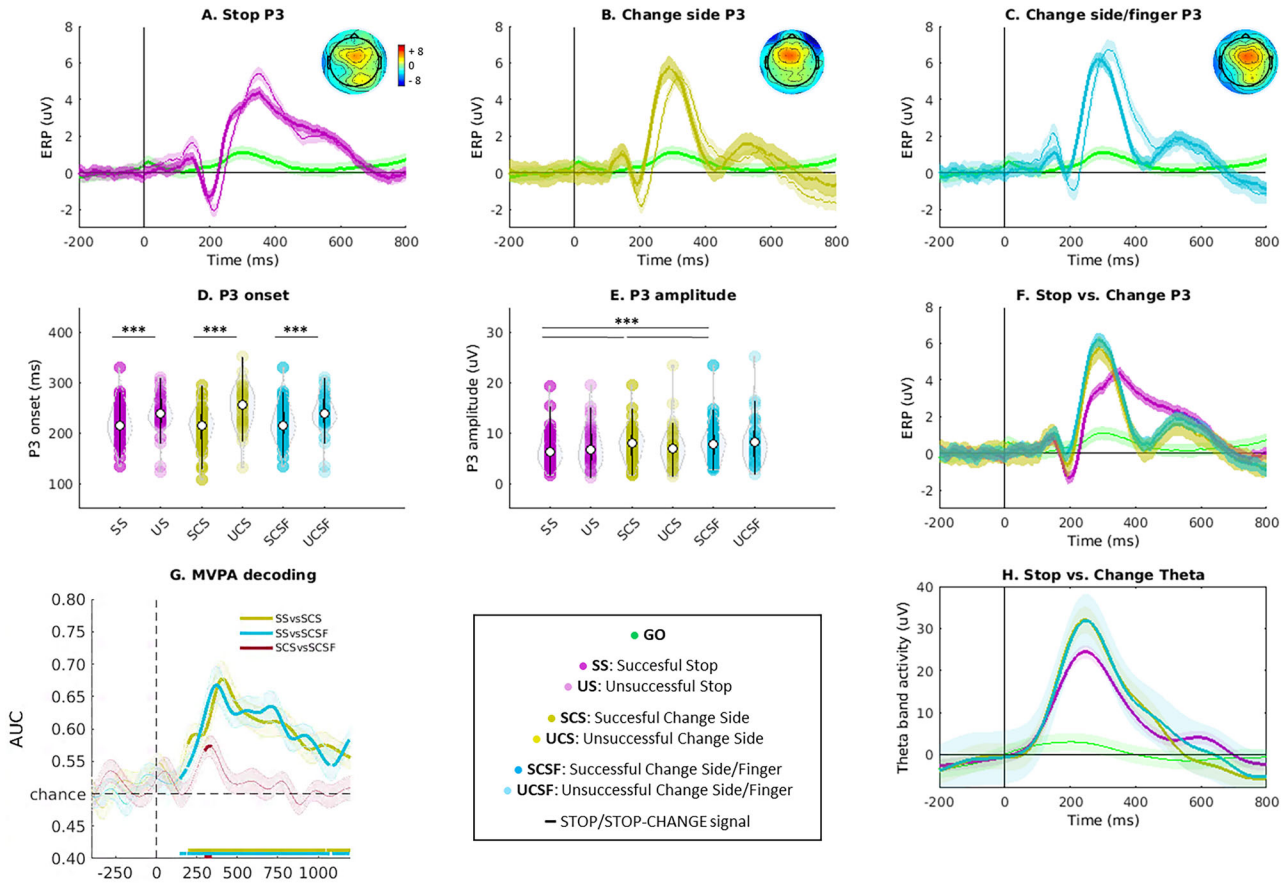

Figure 7. EEG results of Experiments 2 and 3. ***A–C,F***, STOP/STOP-CHANGE signal locked frontocentral grand-average ERP waveforms. Grand-average topographies were computed at the P3 peak latency identified at the group level. ***D,E***, Individual's P3 onset and amplitude. ***G***, Whole-scalp EEG MVPA decoding performances. Horizontal colored lines indicate significant data points (see Materials and Methods). ***H***, Frontocentral θ power time course (grand-average). $*p_{FDR} < 0.05$; $**p_{FDR} < 0.01$; $***p_{FDR} < 0.001$.

revision conditions, with moderate evidence supporting the null hypothesis. This might suggest that directional subcortical–cortical β-bursting associated with the hyperdirect pathway (Torrecillos et al., 2018; Diesburg et al., 2021) is part of a "pause" process that triggers early broad inhibition in a fully nonselective fashion. This speculative proposal would require a more direct investigation of the subcortical dynamic within action revision, including intracranial recording from the STN.

Second, prEMG showed that some motor activation from the aborted initial response survived the "pause"-stage inhibition. This general finding speaks toward the fact that action-stopping may not be carried out by a single process. Our specific hypothesis in the current study was that we would find common prEMG dynamics across action-revision conditions, reflecting a shared "pause" process. In contrast, prEMG trials count, amplitude, and timing scaled across our conditions, indicating that more residual motoric activity escaped inhibition in change-side-and-finger than in change-side and then stop successful trials. As the EMG reflects a net output of the motor system, its properties might actually reflect both the engagement of the "pause" and "cancel" (or "retune"; see below) processes (Fisher et al., 2024), depending on the task demand. Accordingly, the broad motor inhibition triggered early in both stopping and changing by the "pause" process (reflected in early-CSE and β-bursts) might then be sustained (in stopping) or released (in changing) depending on the required revision. This release might thus have led to earlier/larger prEMG in action-changing. Accordingly, we report a prEMG/GO2-RTs correlation and faster GO2-RTs than initial GO-RT. These are compatible with the notion that the earlier release in the motor inhibition of the aborted response facilitates the redirection of the initial motor activation to speed its "retuning." Recent proposals that the "pause" versus "cancel" relative timing varies based on individuals' strategies and task context (Hannah et al., 2022; Pani et al., 2022) might suggest that this quick redirection of the motor activity differs across our experiments. Indeed, a surprising result was that SSRT was much faster for changing than stopping in Experiments 2 and 3, which was not the case in Experiment 1. Although SSRT has been widely criticized as a latent construct (Boucher et al., 2007; Skippen et al., 2019; Huster et al., 2020; Bissett et al., 2021), this difference could reflect a task-design effect on the speed of redirecting the motor command. Indeed, GO and STOP-CHANGE stimuli instructions were associated with a specific symbol (left vs right arrow) in Experiment 1, while they relied on tracking the green target in Experiments 2 and 3. Motor redirection from the aborted initial response to the new one might be speeded in this tracking context. Further investigation using multiple effectors could address this hypothesis, as various effector combinations have been associated with modulations of stopping versus changing SSRT differences (Boecker et al., 2013). Dual-coil TMS assessment of CSE might also provide further insight into this proposed quick transfer of the motor command (Ratcliffe et al., 2022; Wadsley et al., 2023b).

Third, a frontocentral P3 ERP was observed in both action-stopping and action-changing, alongside an earlier P3 onset

latency between successfully and unsuccessfully canceled responses. Beyond the replication of P3 decisive role in successful action-stopping (Kok et al., 2004; Wessel and Aron, 2015; Dykstra et al., 2020; Tatz et al., 2021), Experiments 2 and 3 showed that P3 peak amplitude consistently increased according to the required response revision in an SS→SCS→SCSF order. The maximal decoding performances of the whole-scalp EEG MVPA fell in the same time range, including for the SCS versus SCSF contrast, and $P3_{CHANGE}$ was higher than $P3_{STOP + GO}$. These support further that the P3 was specifically increased in action-changing compared with action-stopping and in changing two response dimensions compared with a single one. Following the view of inhibition being implemented similarly between action-stopping and action-changing (change = stop + reengage; Boecker et al., 2013), one might expect that the "cancel" stage, and P3 as its purported signature, completes the initial-response suppression independently of the new response engagement, though overlapping in time (Verbruggen et al., 2008). In contrast, the P3 modulation we reported may reflect the need for additional cognitive control in action-changing. Based on a "context-updating-theory" of P3-type waveforms (Donchin and Coles, 1988; Polich, 2007), the larger update required in the motor/task representation generated by the primary stimulus could be associated with an increased P3 in action-changing. Higher frontocentral θ power evoked by the STOP-CHANGE versus STOP signal may also pair with higher cognitive demand (Huster et al., 2013; Messel et al., 2021). Therefore, we propose that the revision could be performed by a selective "retuning" of the motor command that results in canceling or redirecting the motoric activity that survived the "pause" inhibition, depending on the task requirements. In favor of this view, previous studies have reported an increased P3 amplitude when an infrequent signal instructed stopping an action compared with continuing it (Tatz et al., 2021; Waller et al., 2021; González-Villar et al., 2022). Our new finding of P3 amplitudes that reflect the amount of response revision is in line with the view of a "pause-then-retune" dynamic triggered by any infrequent event (Wessel and Aron, 2017), the "retune"-stage neurophysiological activity scaling with the required motor-command revision: in the current case, either continuing, stopping, or changing the response. To specify how the motor response retuning is implemented beyond our discrete approach (change-side vs change-side-and-finger), future work might modulate the amount of engaged response change in a continuous fashion, e.g., based on movement trajectory tracking (Zanone and Athènes, 2013; Erb et al., 2016; Hervault et al., 2019; Temprado et al., 2020; London et al., 2021). Moreover, such specific "retuning" of the motor command might specifically engage the pre-SMA, whose role has been previously suggested in reweighting action programs (Jha et al., 2015; Diesburg and Tatz, 2021; Hervault et al., 2022; Wolpe et al., 2022). Although it is still speculative at this stage, this proposal would align with the finding that pre-SMA lesions impaired action-changing to a larger extent than action-stopping (Roberts and Husain, 2015).

In conclusion, we aimed to assess the neurophysiological signatures of human action revision in a previously unseen, comprehensive fashion. Combining EEG, EMG, TMS, and a novel experimental paradigm led to unique insights into the differential dynamics of action-stopping and action-changing. Common and unique neurophysiological processes between action-stopping and action-changing led us to propose that inhibitory control is implemented in a generic "pause-then-retune" dynamic that specifies its mechanism depending on the required response revision.

References

Antons S, Boecker M, Gauggel S, Gordi VM, Patel HJ, Binkofski F, Drueke B (2019) Strategies of selective changing: preparatory neural processes seem to be responsible for differences in complex inhibition. PLoS One 14: e0214652.

Badry R, Mima T, Aso T, Nakatsuka M, Abe M, Fathi D, Foly N, Nagiub H, Nagamine T, Fukuyama H (2009) Suppression of human cortico-motoneuronal excitability during the stop-signal task. Clin Neurophysiol 120:1717–1723.

Bell AJ, Sejnowski TJ (1995) An information-maximization approach to blind separation and blind deconvolution. Neural Comput 7:1129–1159.

Benjamini Y, Krieger AM, Yekutieli D (2006) Adaptive linear step-up procedures that control the false discovery rate. Biometrika 93:491–507.

Bissett PG, Jones HM, Poldrack RA, Logan GD (2021) Severe violations of independence in response inhibition tasks. Sci Adv 7:12.

Bissett PG, Logan GD (2014) Selective stopping? Maybe not. J Exp Psychol Gen 143:455–472.

Boecker M, Buecheler MM, Schroeter ML, Gauggel S (2007) Prefrontal brain activation during stop-signal response inhibition: an event-related functional near-infrared spectroscopy study. Behav Brain Res 176:259–266.

Boecker M, Drueke B, Vorhold V, Knops A, Philippen B, Gauggel S (2011) When response inhibition is followed by response reengagement: an event-related fMRI study. Hum Brain Mapp 32:94–106.

Boecker M, Gauggel S, Drueke B (2013) Stop or stop-change—does it make any difference for the inhibition process? Int J Psychophysiol 87: 234–243.

Boucher L, Palmeri TJ, Logan GD, Schall JD (2007) Inhibitory control in mind and brain: an interactive race model of countermanding saccades. Psychol Rev 114:376–397.

Brainard DH (1997) The psychophysics toolbox. Spat Vis 10:433–436.

Cagnan H, et al. (2019) Temporal evolution of beta bursts in the parkinsonian cortical and basal ganglia network. Proc Natl Acad Sci U S A 116:16095–16104.

Choo Y, Matzke D, Bowren MD Jr, Tranel D, Wessel JR (2022) Right inferior frontal gyrus damage is associated with impaired initiation of inhibitory control, but not its implementation. Elife 11:e79667.

Claffey MP, Sheldon S, Stinear CM, Verbruggen F, Aron AR (2010) Having a goal to stop action is associated with advance control of specific motor representations. Neuropsychologia 48:541–548.

Coxon JP, Stinear CM, Byblow WD (2006) Intracortical inhibition during volitional inhibition of prepared action. J Neurophysiol 95:3371–3383.

De Jong R, Coles MG, Logan DG (1995) Strategies and mechanisms in non-selective and selective inhibitory motor control. J Exp Psychol Hum Percept Perform 21:498–511.

Delorme A, Makeig S (2004) EEGLAB: an open source toolbox for analysis of single-trial EEG dynamics including independent component analysis. J Neurosci Methods 134:9–21.

Diesburg DA, Greenlee JD, Wessel JR (2021) Cortico-subcortical ß burst dynamics underlying movement cancellation in humans. Elife 10:e70270.

Diesburg DA, Tatz JR (2021) Unexpected events activate a frontal-basal-ganglia inhibitory network: what is the role of the pre-supplementary motor area? J Neurosci 41:5135–5137.

Diesburg DA, Wessel JR (2021) The pause-then-cancel model of human action-stopping: theoretical considerations and empirical evidence. Neurosci Biobehav Rev 129:17–34.

Donchin E, Coles MGH (1988) Is the P300 component a manifestation of context updating? Behav Brain Sci 11:357–374.

Drueke B, Boecker M, Schlaegel S, Moeller O, Hiemke C, Gründer G, Gauggel S (2010) Serotonergic modulation of response inhibition and re-engagement? Results of a study in healthy human volunteers. Hum Psychopharmacol 25:472–480.

Duque J, Greenhouse I, Labruna L, Ivry RB (2017) Physiological markers of motor inhibition during human behavior. Trends Neurosci 40:219–236.

Dykstra T, Waller DA, Hazeltine E, Wessel JR (2020) Leveling the field for a fairer race between going and stopping: neural evidence for the race model of motor inhibition from a new version of the stop signal task. J Cogn Neurosci 32:590–602.

Elchlepp H, Verbruggen F (2017) How to withhold or replace a prepotent response: an analysis of the underlying control processes and their temporal dynamics. Biol Psychol 123:250–268.

Enz N, Ruddy KL, Rueda-Delgado LM, Whelan R (2021) Volume of β-bursts, but not their rate, predicts successful response inhibition. J Neurosci 41: 5069–5079.
Erb CD, Moher J, Sobel DM, Song J-H (2016) Reach tracking reveals dissociable processes underlying cognitive control. Cognition 152:114–126.
Fahrenfort JJ, van Driel J, van Gaal S, Olivers CNL (2018) From ERPs to MVPA using the Amsterdam decoding and modeling toolbox (ADAM). Front Neurosci 12:368.
Fisher M, Trinh H, O'Neill J, Greenhouse I (2024) Early rise and persistent inhibition of electromyography during failed stopping. J Cogn Neurosci 36:1412–1426.
Giarrocco F, Bardella G, Giamundo M, Fabbrini F, Brunamonti E, Pani P, Ferraina S (2021) Neuronal dynamics of signal selective motor plan cancellation in the macaque dorsal premotor cortex. Cortex 135:326–340.
González-Villar A, Galdo-Álvarez S, Carrillo-de-la-Peña MT (2022) Neural correlates of unpredictable stop and non-stop cues in overt and imagined execution. Psychophysiology 59:e14019.
Hannah R, Jana S, Muralidharan V (2022) Does action-stopping involve separate pause and cancel processes? A view from premotor cortex. Cortex 152:157–159.
Hannah R, Muralidharan V, Sundby KK, Aron AR (2020) Temporally-precise disruption of prefrontal cortex informed by the timing of beta bursts impairs human action-stopping. Neuroimage 222:117222.
Hervault M, Huys R, Farrer C, Buisson JC, Zanone PG (2019) Cancelling discrete and stopping ongoing rhythmic movements: do they involve the same process of motor inhibition? Hum Mov Sci 64:296–306.
Hervault M, Soh C, Wessel JR (2025) Does the stop-signal P3 reflect inhibitory control? Cortex 183:232–250.
Hervault M, Zanone P-G, Buisson J-C, Huys R (2022) Multiple brain sources are differentially engaged in the inhibition of distinct action types. J Cogn Neurosci 34:258–272.
Huster RJ, Enriquez-Geppert S, Lavallee CF, Falkenstein M, Herrmann CS (2013) Electroencephalography of response inhibition tasks: functional networks and cognitive contributions. Int J Psychophysiol 87:217–233.
Huster RJ, Messel MS, Thunberg C, Raud L (2020) The P300 as marker of inhibitory control – fact or fiction? Cortex 132:334–348.
Hynd M, Soh C, Rangel BO, Wessel JR (2021) Paired-pulse TMS and scalp EEG reveal systematic relationship between inhibitory GABAa signaling in M1 and fronto-central cortical activity during action stopping. J Neurophysiol 125:648–660.
Jana S, Hannah R, Muralidharan V, Aron AR (2020) Temporal cascade of frontal, motor and muscle processes underlying human action-stopping. Elife 9:e50371.
Jha A, Nachev P, Barnes G, Husain M, Brown P, Litvak V (2015) The frontal control of stopping. Cereb Cortex 25:4392–4406.
Kenner NM, Mumford JA, Hommer RE, Skup M, Leibenluft E, Poldrack RA (2010) Inhibitory motor control in response stopping and response switching. J Neurosci 30:8512–8518.
Kok A, Ramautar JR, De Ruiter MB, Band GPH, Ridderinkhof KR (2004) ERP components associated with successful and unsuccessful stopping in a stop-signal task. Psychophysiology 41:9–20.
Krämer UM, Knight RT, Münte TF (2011) Electrophysiological evidence for different inhibitory mechanisms when stopping or changing a planned response. J Cogn Neurosci 23:2481–2493.
Krekelberg B (2023) bayesFactor. Available at: https://github.com/klabhub/bayesFactor
Logan GD, Burkell J (1986) Dependence and independence in responding to double stimulation: a comparison of stop, change, and dual-task paradigms. J Exp Psychol Hum Percept Perform 12:549–563.
Logan GD, Cowan WB (1984) On the ability to inhibit thought and action: a theory of an act of control. Psychol Rev 91:295–327.
London D, Fazl A, Katlowitz K, Soula M, Pourfar MH, Mogilner AY, Kiani R (2021) Distinct population code for movement kinematics and changes of ongoing movements in human subthalamic nucleus. Elife 10:e64893.
Majid DSA, Cai W, George JS, Verbruggen F, Aron AR (2012) Transcranial magnetic stimulation reveals dissociable mechanisms for global versus selective corticomotor suppression underlying the stopping of action. Cereb Cortex 22:363–371.
Maris E, Oostenveld R (2007) Nonparametric statistical testing of EEG- and MEG-data. J Neurosci Methods 164:177–190.
McClure EB, Treland JE, Snow J, Schmajuk M, Dickstein DP, Towbin KE, Charney DS, Pine DS, Leibenluft E (2005) Deficits in social cognition and response flexibility in pediatric bipolar disorder. Am J Psychiatry 162:1644–1651.
Messel MS, Raud L, Hoff PK, Stubberud J, Huster RJ (2021) Frontal-midline theta reflects different mechanisms associated with proactive and reactive control of inhibition. Neuroimage 241:118400.
Nikolov P, Hassan SS, Schnitzler A, Groiss SJ (2021) Influence of high pass filter settings on motor evoked potentials. Front Neurosci 15: 665258.
Pani P, Giarrocco F, Bardella G, Brunamonti E, Ferraina S (2022) Reply to: Hannah et al. (2021) commentary: 'does action-stopping involve separate pause and cancel processes? A view from premotor cortex': action-stopping models must consider the role of the dorsal premotor cortex. Cortex 152:160–163.
Pion-Tonachini L, Kreutz-Delgado K, Makeig S (2019) ICLabel: an automated electroencephalographic independent component classifier, dataset, and website. Neuroimage 198:181–197.
Polich J (2007) Updating P300: an integrative theory of P3a and P3b. Clin Neurophysiol 118:2128–2148.
Rangel-Gomez M, Knight RT, Krämer UM (2015) How to stop or change a motor response: Laplacian and independent component analysis approach. Int J Psychophysiol 97:233–244.
Ratcliffe CE, McAllister CJ, MacDonald HJ (2022) Dual-coil transcranial magnetic stimulation reveals temporal dynamics of bilateral corticomotor excitability during response inhibition. 2022.09.14.507942. Available at: https://www.biorxiv.org/content/10.1101/2022.09.14.507942v1
Raud L, Huster RJ, Ivry RB, Labruna L, Messel MS, Greenhouse I (2020) A single mechanism for global and selective response inhibition under the influence of motor preparation. J Neurosci 40:7921–7935.
Raud L, Thunberg C, Huster RJ (2022) Partial response electromyography as a marker of action stopping. Elife 11:e70332.
Roberts RE, Husain M (2015) A dissociation between stopping and switching actions following a lesion of the pre-supplementary motor area. Cortex 63:184–195.
Rossi S, Hallett M, Rossini PM, Pascual-Leone A (2011) Screening questionnaire before TMS: an update. Clin Neurophysiol 122:1686.
Rossini PM, et al. (1994) Non-invasive electrical and magnetic stimulation of the brain, spinal cord and roots: basic principles and procedures for routine clinical application. Report of an IFCN committee. Electroencephalogr Clin Neurophysiol 91:79–92.
Schmidt R, Berke JD (2017) A pause-then-cancel model of stopping: evidence from basal ganglia neurophysiology. Philos Trans R Soc Lond B Biol Sci 372:20160202.
Skippen P, Fulham WR, Michie PT, Matzke D, Heathcote A, Karayanidis F (2020) Reconsidering electrophysiological markers of response inhibition in light of trigger failures in the stop-signal task. Psychophysiology 57: e13619.
Skippen P, Matzke D, Heathcote A, Fulham WR, Michie P, Karayanidis F (2019) Reliability of triggering inhibitory process is a better predictor of impulsivity than SSRT. Acta Psychol 192:104–117.
Tatz JR, Mather A, Wessel JR (2023) β-Bursts over frontal cortex track the surprise of unexpected events in auditory, visual, and tactile modalities. J Cogn Neurosci 35:485–508.
Tatz JR, Soh C, Wessel JR (2021) Common and unique inhibitory control signatures of action-stopping and attentional capture suggest that actions are stopped in two stages. J Neurosci 41:8826–8838.
Temprado J-J, Torre MM, Langeard A, Julien-Vintrou M, Devillers-Réolon L, Sleimen-Malkoun R, Berton E (2020) Intentional switching between bimanual coordination patterns in older adults: is it mediated by inhibition processes? Front Aging Neurosci 12:29.
Torrecillos F, et al. (2018) Modulation of beta bursts in the subthalamic nucleus predicts motor performance. J Neurosci 38:8905–8917.
van den Wildenberg WPM, Ridderinkhof KR, van Wouwe NC, Neimat JS, Bashore TR, Wylie SA (2017) Overriding actions in Parkinson's disease: impaired stopping and changing of motor responses. Behav Neurosci 131:372–384.
van den Wildenberg WPM, van Wouwe NC, Ridderinkhof KR, Neimat JS, Elias WJ, Bashore TR, Wylie SA (2021) Deep-brain stimulation of the subthalamic nucleus improves overriding motor actions in Parkinson's disease. Behav Brain Res 402:113124.
Verbruggen F, et al. (2019) A consensus guide to capturing the ability to inhibit actions and impulsive behaviors in the stop-signal task. Elife 8: e46323.

Verbruggen F, Logan GD (2009) Models of response inhibition in the stop-signal and stop-change paradigms. Neurosci Biobehav Rev 33: 647–661.

Verbruggen F, Schneider DW, Logan GD (2008) How to stop and change a response: the role of goal activation in multitasking. J Exp Psychol Hum Percept Perform 34:1212–1228.

Wadsley CG, Cirillo J, Nieuwenhuys A, Byblow WD (2023a) A global pause generates nonselective response inhibition during selective stopping. Cereb Cortex 33:9729–9740.

Wadsley CG, Cirillo J, Nieuwenhuys A, Byblow WD (2023b) Proactive interhemispheric disinhibition supports response preparation during selective stopping. J Neurosci 43:1008–1017.

Waller DA, Hazeltine E, Wessel JR (2021) Common neural processes during action-stopping and infrequent stimulus detection: the frontocentral P3 as an index of generic motor inhibition. Int J Psychophysiol 163: 11–21.

Wessel JR (2020) β-Bursts reveal the trial-to-trial dynamics of movement initiation and cancellation. J Neurosci 40:411–423.

Wessel JR, Aron AR (2015) It's not too late: the onset of the frontocentral P3 indexes successful response inhibition in the stop-signal paradigm. Psychophysiology 52:472–480.

Wessel JR, Aron AR (2017) On the globality of motor suppression: unexpected events and their influence on behavior and cognition. Neuron 93:259–280.

Wessel JR, Diesburg DA, Chalkley NH, Greenlee JDW (2022) A causal role for the human subthalamic nucleus in non-selective cortico-motor inhibition. Curr Biol 32:3785–3791.e3.

Wessel JR, Reynoso HS, Aron AR (2013) Saccade suppression exerts global effects on the motor system. J Neurophysiol 110:883–890.

Wickens TD (2002) *Elementary signal detection theory*. New York, NY, US: Oxford University Press.

Wolpe N, Hezemans FH, Rae CL, Zhang J, Rowe JB (2022) The pre-supplementary motor area achieves inhibitory control by modulating response thresholds. Cortex 152:98–108.

Zanone P-G, Athènes S (2013) Switching among graphic patterns is governed by oscillatory coordination dynamics: implications for understanding handwriting. Front Psychol 4:662.